A MATHEMATICAL MODEL AND OPTIMIZATION OF THE STRUCTURE FOR POROUS AIR ELECTRODES

M. VIITANEN and M. J. LAMPINEN*

Helsinki University of Technology, Department of Energy Engineering, Otakaari 4, SF-02150 Espoo (Finland)

(Received February 16, 1990)

Summary

A mathematical model for porous air electrodes is developed to optimize the structure of the electrode. The electrode consists of two layers; a gas-supplying layer and a reaction layer. The reaction layer is assumed to consist of porous catalytical agglomerates surrounded by a hydrophobic gas-supplying zone, which is made from the same material as the gas-supplying layer. It is assumed in the model that these agglomerates have a cylindrical shape. The model takes into account the diffusion of oxygen in the gas-supplying layer, the diffusion of dissolved oxygen, the electrochemical reactions taking place, ionic ohmic drop in the cylinder and also electronic ohmic drop due to the finite conductivity of solid material.

To calculate a polarization curve altogether 13 parameters must be known; four geometrical parameters, six parameters which are characteristic of the electrode and three parameters which determine the experimental conditions. The performance of the air electrode is calculated for different geometries and the optimum geometry is determined. In order to simulate a real air electrode the characteristic parameters are measured. Comparisons have also been made between calculated and measured polarization curves.

1. Introduction

Teflon bonded gas diffusion electrodes made in our laboratory consist of two layers: a porous hydrophobic gas-supplying layer, which has good conductivity, and a reaction layer, which is partly hydrophobic and partly hydrophilic. A schematic representation of the structure of a real electrode is presented in Fig. 1.

The gas-supplying layer consists of porous and hydrophobic material, so that the reactant gas, oxygen, can easily diffuse through the pores towards the reaction layer, where reactions take place. The hydrophobic property of

---

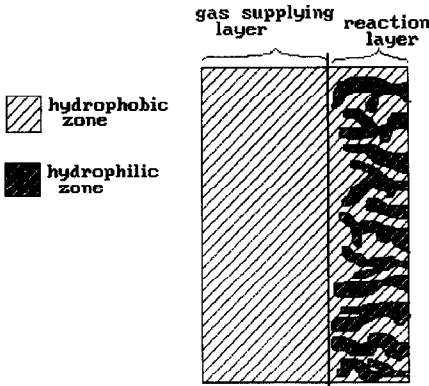*Author to whom correspondence should be addressed.

Fig. 1. Air electrode.

the material is very important; it prevents the electrolyte from penetrating into the pores. Electrolyte in the pores would prevent the diffusion of oxygen to the reaction layer and this would result in a dramatic deterioration of the electrode's performance.

The hydrophobic zone in the reaction layer is the same material as the gas-supplying layer, and the hydrophilic zone consists of agglomerates of catalytical particles. These agglomerates are porous and are flooded with electrolyte.

In the mathematical model the agglomerates of catalytical particles are described as cylinders whose axes are perpendicular to the surface of the electrode. Hereafter, when considering the reaction layer, we often use the word 'cylinder' in this connection. The radius of a cylinder is r_0 and the length is x_0. The mathematical model of the electrode consists of equal elements which are located in a two-dimensional array. Each element is composed of a cylinder, a hydrophobic zone which surrounds the cylinder and a part of the gas-supplying layer whose thickness is d_0. The hydrophobic zone which surrounds the cylinder has an intersection area of S. The model of the electrode is presented in Fig. 2(a) and an element of the model electrode in Fig. 2(b).

During the operation of the electrode, oxygen gas diffuses through the gas-supplying layer towards the hydrophobic zone of the reaction layer, dissolves in the electrolyte contained in the cylinder and then reacts on the active sites of catalyst particles. The generated ionic current is conducted towards the free electrolyte in an axial direction of the cylinder. These processes are also presented in Fig. 2(b).

The model was originally presented by Giner and Hunter [1] and later improved by Iliev et al. [2]. We have improved the model further by introducing the electronic IR drop and by developing a computer program which calculates polarization curves, and which is used to optimize the structure of the air electrode, to simulate a real air electrode and to analyze the different factors affecting the performance of the electrode. The aim of this model

gas supplying reaction
layer | layer

an element
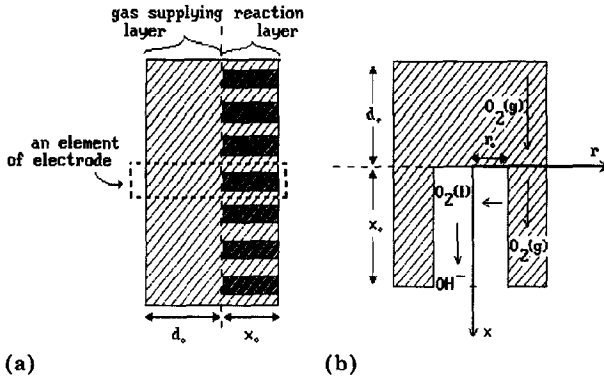of electrode

d_o x_o

(a)   (b)

Fig. 2. The model of the electrode.

and program is to contribute to the understanding of the working mechanism of the porous air electrodes and to serve as an aid in manufacturing air electrodes.

2. The assumptions of the model

The model takes into account the physical structure of the electrode, the main transport processes which take place, the main electrochemical processes and also ionic ohmic drop in the cylinder and electronic ohmic drop due to the finite conductivity of material.

We assume in the model that the hydrophobic zone both in the gas-supplying layer and in the reaction layer is homogeneous. The catalyst particles and electrolyte are also homogeneously dispersed in the cylinder. The activity of the catalyst particles is also constant throughout the cylinder.

The void fraction β is defined as the ratio of the cross-sectional area S and the cross-sectional area of the element. The number of elements per unit surface area, N, is related to the void fraction as follows

$$\beta = \frac{S}{S + \pi r_0^2} = 1 - N\pi r_0^2 \tag{1}$$

The cylindrical coordinates are used in the model. The x-axis is perpendicular to the surface of the electrode, the length of cylinder is x_0, so at the bottom of the cylinder $x = 0$. At the center of the cylinder $r = 0$, and the radius of the cylinder is r_0.

Next we shall discuss transport processes in the gas diffusion electrode. The oxygen diffuses through the gas-supplying layer. It is assumed that the diffusion occurs only in the direction of the x-axis (Fig. 2(b)). This assumption is also used in the hydrophobic zone which surrounds the cylinder; we suppose that this zone is so thin that when oxygen dissolves in the electrolyte, the concentration gradient in the r-direction remains zero.

The effective diffusion coefficient in the hydrophobic zone is denoted by $\bar{D}_g$.

The dissolution of oxygen is assumed to be a fast process, so that on the surface of the cylinder the local concentration of oxygen on the electrolyte side is proportional to the partial pressure of oxygen on the gas side. This means that Henry's law, $C(r_0,x) = kP(x)$ is valid in the vicinity of the surface. The concentration of oxygen in the electrolyte is denoted by $C(r,x)$ and the partial pressure of oxygen by $P(x)$.

In the cylinder, oxygen diffuses only radially inwards and reacts on the diffusion path. The concentration $C(r,x)$ depends on the diffusion in the hydrophobic zone, on the effective diffusion coefficient in the cylinder, $\bar{D}_e$, and on the rate of the electrochemical reaction.

The electrochemical reaction which takes place in the cylinder is assumed to be of the first order. The overall reaction is

$$O_2 + 2H_2O + 4e^- \longrightarrow 4OH^-$$
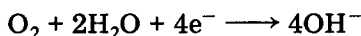
The generated current is a function of the concentration of oxygen and overpotentials $\eta(x)$ and $\eta_m(x)$, which are the ionic and electronic potential drop, respectively. These are assumed only to be functions of x. These overpotentials will be defined precisely and discussed in more detail in connection with ionic and electronic IR drops. Equation (2) describes the local current density per unit surface area of catalyst

$$i(r,x) = i_0 \frac{C(r,x)}{C_0} \exp\left(\frac{\alpha z F}{RT} (\eta(x) - \eta_m(x))\right) \tag{2}$$

where i_0 is the exchange current density per unit surface of the catalyst, C_0 ($= kP_0$) is the solubility of oxygen at bulk gas pressure, P_0, α is the transfer coefficient, z is the stoichiometric number, F is the Faraday constant, R is the gas constant and T is temperature. Equation (2) will be derived later by eqn. (18).

The generated ionic current $j(x)$ flows towards the free electrolyte along the x-axes and is given by the expression

$$j(x) = \int_0^x \int_0^r \gamma i(r,x) 2\pi r \, dr \, dx \tag{3}$$

where γ is the ratio of catalyst surface area to catalyst volume. The total current density can be calculated using Ohm's law, $j = \bar{\kappa}E$, where $\bar{\kappa}$ is the effective conductivity of the electrolyte in the cylinder and E is the strength of the electric field. Since we have assumed that overpotential is only a function of the x-coordinate, $E = -(d\eta(x)/dx)$, and because the cross section through which the ionic current flows is πr_0^2, we get from Ohm's law

$$j(x) = -\bar{\kappa}\pi r_0^2 \frac{d\eta(x)}{dx} \tag{4}$$

Since the number of cylinders per unit surface area is N, the total current density, I, whose positive direction is opposite to the x-axis, is

$$I = -Nj(x_0) \tag{5}$$

and using eqns. (1) and (4), we can express the total current density by

$$I = \frac{1-\beta}{\pi r_0^2} j(x_0) = (1-\beta)\bar{\kappa} \left(\frac{d\eta(x)}{dx}\right)_{x=x_0} \tag{6}$$

We assume that there is no convection of electrolyte in the cylinder, or at least that it is so small that it does not affect the ionic current and it can therefore be ignored.

In addition to the ionic IR drop, electronic IR drop is also considered. So the change in overpotential is due to ionic IR drop as well as to the electronic IR drop. In a later section we will discuss how to take into account the electronic IR drop.

3. Equations for the transport of oxygen

3.1. The gas-supplying layer

Since we are considering the steady state operation, the partial pressure of oxygen throughout the electrode is constant *versus* time. This means that the flux of oxygen, J, is constant along the x-coordinate (because from Fick's second law $(dP/dt) = -D(dJ/dx)$). The partial pressure of oxygen can be calculated from Fick's first law, which can be written in this case as follows

$$J(x) = -\bar{D}_g \frac{\Delta P(x)}{\Delta x} \tag{7}$$

where $\bar{D}_g$ (mol/(Pa m s)) is the effective diffusion coefficient of oxygen. Because the flux is related to the total current density according to equation $J = I/(4F)$, the partial pressure of oxygen at the boundary of the reaction layer, where $x = 0$, can be calculated from

$$P(x = 0) = P_1(I) = P_0 \left\{1 - \frac{Id_0}{4F\bar{D}_g P_0}\right\} \tag{8}$$

This equation can be combined with eqn. (6), which gives the relation between the total current density and the gradient of overpotential at $x = x_0$.

Equation (8) can also be used to calculate the limiting current density. This is the maximum current density which is reached when the partial pressure of oxygen is so small (close to zero) in the reaction layer that no further reaction can occur. In the mathematical model of the electrode this limit is reached when the partial pressure of oxygen at $x = 0$ is zero. From eqn. (8) the limiting current density can be calculated by setting $P_1(I) = 0$

$$I_{\text{lim}} = \frac{4F\bar{D}_g P_0}{d_0} \tag{9}$$

3.2. The hydrophobic zone of the reaction layer

Here we must also consider the dissolution of oxygen at the surface of the cylinder. The flux of oxygen across the surface is determined by the concentration gradient of oxygen on the electrolyte side, because it is assumed that the dissolution itself is a rapid process. The flux across the circumference of the cylinder is

$$J(x) = -2\pi r_0 \bar{D}_e \left(\frac{\partial C}{\partial r}\right)_{r = r_0} \tag{10}$$

where $\bar{D}_e$ is the effective diffusion coefficient of oxygen in the cylinder and $C = C(r,x)$ is the concentration of oxygen in the cylinder. The partial pressure of oxygen in the hydrophobic zone of the reaction layer can now be expressed by

$$S\bar{D}_g \frac{d^2 P}{dx^2} - 2\pi r_0 \bar{D}_e \left(\frac{\partial C}{\partial r}\right)_{r = r_0} = 0 \tag{11}$$

One boundary condition for the partial pressure $P(x)$ has already been derived, eqn. (8), which gives the partial pressure at $x = 0$. The other boundary condition is

$$\left(\frac{dP}{dx}\right)_{x = x_0} = 0 \tag{12}$$

which means that the oxygen gas flow at $x = x_0$ is zero.

3.3. The cylinder

On the diffusion path oxygen is consumed due to the electrochemical reaction $(O_2 + 2H_2O + 4e^- \Rightarrow 4OH^-)$. The reaction density expressed with the aid of the current is $i\gamma/(4F)$ $(\text{mol}/(\text{m}^3 \text{ s}))$. For the cylindrical diffusion it can be written

$$\bar{D}_e \frac{\partial^2 C(r,x)}{\partial r^2} + \bar{D}_e \frac{1}{r} \frac{\partial C(r,x)}{\partial r} - \frac{\gamma i(r,x)}{4F} = 0 \tag{13}$$

Because the dissolution is a rapid process, the other boundary condition for the concentration is

$$C(r_0,x) = kP(x) \tag{14}$$

And the other follows from symmetry

$$\left(\frac{\partial C}{\partial r}\right)_{r = 0} = 0 \tag{15}$$

4. Ionic and electronic *IR* drop

In Fig. 3 a schematic drawing of the potential curves in the electrode as a function of the x-coordinate is presented. In the reaction layer, where $0 \leqslant x \leqslant x_0$, there are two potential curves; $\phi_L(x)$, potential in the liquid phase and $\phi_M(x)$, potential in the solid material phase. The measurable overpotential is

$$\eta(x) = \phi_{ref} - \phi_1 = (\phi_L(x) - \phi_{M_0}) + C_1 + C_2 \tag{16}$$

where C_1 and C_2 are constants, ϕ_1 is the potential at the air electrode (at the inlet $x = -d_0$) and ϕ_{ref} is the potential of the reference electrode. The overpotential due to the electronic *IR* drop is

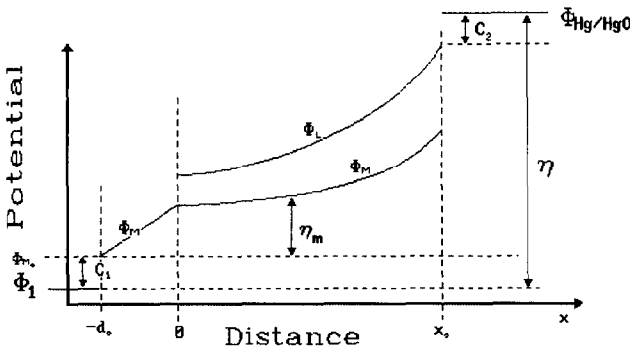$$\eta_m(x) = \phi_M(x) - \phi_{M_0} \tag{17}$$

Fig. 3. The potential curves in the air electrode.

4.1. The local current density

The local current density is defined by

$$i(r,x) = i'_0 \frac{C(r,x)}{C_0} \exp\left(\frac{\alpha z F}{RT} (\phi_L(x) - \phi_M(x))\right) \tag{18}$$

From eqns. (16) and (17) we obtain $\phi_L(x) - \phi_M(x) = \eta(x) - \eta_m(x) + C_1 + C_2$. Substituting this in eqn. (18) and then using the notation

$$i_0 = i'_0 \exp(\alpha z F/(RT)(C_1 + C_2)) \tag{19}$$

we obtain the previously presented equation (eqn. (2)).

4.2. Equations for electronic and ionic IR drop

We assume that electrons transmit the hydrophobic zone and reaction layer only in the direction of the x-axes. In other words, the electrons are moved to the cylinder with no voltage drop in the direction perpendicular to the x-axes. This is quite similar to the assumption that when oxygen

dissolves through the surface of the cylinder, the concentration gradient of oxygen perpendicular to the x-axes remains zero.

In the steady state the sum of electronic current (j_M) and ionic current (j_L) is constant

$$j_L(x) + j_M(x) = \text{constant} \tag{20}$$

Using Ohm's law the currents can be written as follows

$$j_L(x) = -\pi r_0^2 \bar{\kappa} \frac{d\phi_L}{dx} \tag{21}$$

$$j_M(x) = -S\bar{\kappa}_m \frac{d\phi_M}{dx} \tag{22}$$

where S is the cross-sectional area of the hydrophobic zone around the cylinder. In these last two equations η and η_m can be used instead of ϕ_L and ϕ_M, respectively, since the derivatives of these are the same. This can easily be seen from eqns. (16) and (17), since the difference between η and ϕ_L and also between η_m and ϕ_M is constant.

When eqns. (20), (21) and (22) are differentiated and η and η_m are used instead of ϕ_L and ϕ_M, respectively, we get

$$\frac{dj_L}{dx} + \frac{dj_M}{dx} = 0 \tag{23}$$

$$\frac{dj_L}{dx} = -\pi r_0^2 \bar{\kappa} \frac{d^2\eta}{dx^2} \tag{24}$$

$$\frac{dj_M}{dx} = -S\bar{\kappa}_m \frac{d^2\eta_m}{dx^2} \tag{25}$$

If the term dj_L/dx in eqn. (24) is divided by $(4F)$, we get the change of flux of OH^- ions across a layer which has a thickness of dx. The change of OH^- ions flux is due to the generation of OH^- ions which is equal to the flux of oxygen through the surface of the cylinder. Hence we can write

$$\frac{dj_L}{dx} \frac{1}{4F} = -2\pi r_0 \bar{D}_e \left(\frac{\partial C}{\partial r}\right)_{r=r_0} \tag{26}$$

Combining eqns. (24) and (26) we get

$$\frac{d^2\eta}{dx^2} - 8\frac{F\bar{D}_e}{\bar{\kappa} r_0} \left(\frac{\partial C}{\partial r}\right)_{r=r_0} = 0 \tag{27}$$

Next we will derive a similar equation for the overpotential in solid materials, η_m. An expression for (dj_M/dx) can be obtained from eqns. (23) and (26). According to eqn. (23) $(dj_L/dx) = -(dj_M/dx)$ and substituting this in eqn. (26), we get

$$\frac{\mathrm{d}j_{\mathrm{M}}}{\mathrm{d}x}\frac{1}{4F} = 2\pi r_0 \bar{D}_{\mathrm{e}}\left(\frac{\partial C}{\partial r}\right)_{r=r_0} \tag{28}$$

Now combining eqns. (25) and (28) we get

$$\frac{\mathrm{d}^2\eta_{\mathrm{m}}}{\mathrm{d}x^2} + 8\frac{\pi r_0 F \bar{D}_{\mathrm{e}}}{\bar{\kappa}_{\mathrm{m}} S}\left(\frac{\partial C}{\partial r}\right)_{r=r_0} = 0 \tag{29}$$

4.3. Boundary conditions

One boundary condition for overpotential in the cylinder is related to the total current density. According to eqn. (6) the total current density can be expressed using the gradient of overpotential at $x = x_0$. When the total current density is known, we get a boundary condition for $\eta(x)$

$$\left(\frac{\mathrm{d}\eta}{\mathrm{d}x}\right)_{x=x_0} = \frac{I}{(1-\beta)\bar{\kappa}} \tag{30}$$

The other boundary condition is

$$\left(\frac{\mathrm{d}\eta}{\mathrm{d}x}\right)_{x=0} = 0 \tag{31}$$

This means that at the bottom of the cylinder, where $x = 0$, the current, $j_{\mathrm{L}}(0)$, is zero.

In the gas-supplying layer, where $-d_0 \leqslant x \leqslant 0$, j_{L} is zero and the electronic current per one element of the model electrode can be expressed by Ohm's equation

$$j_{\mathrm{M}}(x) = -\bar{\kappa}_{\mathrm{m}}(S + \pi r_0^2)\frac{\mathrm{d}\phi_{\mathrm{M}}}{\mathrm{d}x} \tag{32}$$

By integrating this equation, we obtain an expression for $\phi_{\mathrm{M}}(0) - \phi_{\mathrm{M}_0}$, (which is η_{m} as defined with eqn. (17))

$$\eta_{\mathrm{m}}(0) = -\frac{d_0 j_{\mathrm{M}}(0)}{\bar{\kappa}_{\mathrm{m}}(S + \pi r^2)} \tag{33}$$

Since the total current density $I = j_{\mathrm{M}}(0)$ and $N(S + \pi r_0^2) = 1$ we get a boundary condition

$$\eta_{\mathrm{m}}(0) = -\frac{Id_0}{\bar{\kappa}_{\mathrm{m}}} \tag{34}$$

In the reaction layer at $x = 0$ the electronic current can be written

$$j_{\mathrm{M}}(0) = -\bar{\kappa}_{\mathrm{m}}S\left(\frac{\mathrm{d}\eta_{\mathrm{m}}}{\mathrm{d}x}\right)_{x=0} \tag{35}$$

As mentioned before $j_L(0)$ is zero, so the total current density is $I = Nj_M(0)$ and since $SN = \beta$, we get the other boundary condition

$$\left(\frac{\mathrm{d}\eta_m}{\mathrm{d}x}\right)_{x=0} = \frac{I}{\beta \bar{\kappa}_m} \tag{36}$$

We now have four eqns. ((11), (13), (27) and (29)) and eight boundary conditions ((8), (12), (14), (15), (30), (31), (34) and (36)), which describe the transport of oxygen, electrochemical reaction and electronic and ionic IR drop. Overpotential η and η_m can be calculated from these equations, when all 13 parameters ($\bar{D}_g$, $\bar{D}_e$, $\bar{\kappa}$, $\bar{\kappa}_m$, γi_0, α, P_0, k, T, x_0, r_0, d_0, β) and the total current density (I) are known.

5. Solving the equations

The concentration of oxygen in the cylinder has a solution under boundary conditions (14) and (15)

$$C(r,x) = kP(x) \frac{I_0(q(x)(r/r_0))}{I_0(q(x))} \tag{37}$$

where I_0 is the modified Bessel function of zero order and

$$q(x) = \left\{ \frac{\gamma i_0 r_0^2}{4F\bar{D}_e C_0} \exp\left[\frac{\alpha zF}{RT}(\eta(x) - \eta_m(x))\right] \right\}^{1/2} \tag{38}$$

From eqn. (37) we get

$$\left(\frac{\partial C}{\partial r}\right)_{r=r_0} = k \frac{q(x)}{r_0} \frac{I_1(q(x))}{I_0(q(x))} P(x) \tag{39}$$

where I_1 is the modified Bessel function of the first order. If the derivative of the concentration in eqns. (11), (27) and (29) is replaced by eqn. (39), we get

$$S\bar{D}_g \frac{\mathrm{d}^2 P}{\mathrm{d}x^2} - 2\pi r_0 \bar{D}_e \frac{k}{r_0} \left\{ q(x) \frac{I_1(q(x))}{I_0(q(x))} \right\} P(x) = 0 \tag{40}$$

$$\frac{\mathrm{d}^2 \eta}{\mathrm{d}x^2} - 8 \frac{F\bar{D}_e}{\bar{\kappa} r_0} \frac{k}{r_0} \left\{ q(x) \frac{I_1(q(x))}{I_0(q(x))} \right\} P(x) = 0 \tag{41}$$

$$\frac{\mathrm{d}^2 \eta_m}{\mathrm{d}x^2} + 8 \frac{\pi r_0 F\bar{D}_e}{\bar{\kappa}_m S} \frac{k}{r_0} \left\{ q(x) \frac{I_1(q(x))}{I_0(q(x))} \right\} P(x) = 0 \tag{42}$$

The partial pressure of oxygen can be solved by eliminating term qI_1/I_0 from eqns. (40) and (41) and integrating the obtained equation twice. The result is

$$P(x) = P_0 - \left\{ \left[\frac{(1-\beta)\bar{\kappa}d_0}{4F\bar{D}_g} + \frac{(1-\beta)\bar{\kappa}}{\beta 4F\bar{D}_g}x \right] \left(\frac{\partial \eta}{\partial x} \right)_{x=x_0} - \frac{(1-\beta)\bar{\kappa}}{\beta 4F\bar{D}_g}(\eta(x)-\eta(0)) \right\}$$

(43)

Substituting eqn. (43) in eqns. (41) and (42), we obtain two equations with two unknown functions, $\eta(x)$ and $\eta_m(x)$. These equations are quite complicated, since $q(x)$ is a function of both $\eta(x)$ and $\eta_m(x)$ (eqn. (38)). These equations are solved numerically using a shooting method. In the following we give a brief summary of the numerical solution method.

The x-axis from zero to x_0 is divided into 101 points, x_i, where $i = 0 \ldots 100$. The second derivative is written as $[(\eta_{i-1} - 2\eta_i + \eta_{i+1})]/\Delta x^2$, where $\eta_i = \eta(x_i)$ and $\Delta x = x_0/100$. If η_0 and η_1 or η_{99} and η_{100} were known, then the third point and the rest of the curve could be calculated explicitly. However, as was mentioned above, η_m is also included in eqn. (41) and η is included in eqn. (42). Thus, to calculate point η_i we have to know η_{i-1}, η_{i-2} and $\eta_{m,i}$, and analogously to calculate point $\eta_{m,i}$, we have to know $\eta_{m,i-1}$, $\eta_{m,i-2}$ and η_i. This means that these two eqns. (41) and (42) must be solved simultaneously.

From the boundary conditions (eqns. (30), (31), (34) and (36)), we know the derivatives of $\eta(x)$ at $x = 0$ and at $x = x_0$, and we know the value of η_m at $x = 0$ as well as the derivative at that point. The problem is how the third point (η_2) can be calculated. To do this we should know $\eta(0)$, but since this is unknown we must make a 'random' choice for this value and then we are able to calculate the whole curve. The proper result must satisfy the boundary condition (30), which is the derivative of η at $x = x_0$. Thus, we must make choices for $\eta(0)$ repeatedly until the correct result is obtained.

The correct value for $\eta(0)$ can be found as follows. We can form a function, which is the difference between the derivative of the calculated curve and the real derivative as a function of $\eta(0)$. Thus, if the derivative of the calculated curve is smaller than the real derivative, the function has a positive value and vice versa. Now the real value of $\eta(0)$ is the root of this function. When the root is found, the equations of $\eta(x)$ and $\eta_m(x)$ ((41) and (42)) are solved and the measurable overpotential is $\eta(x_0)$.

6. The experimental determination of the parameters

There are 13 parameters which must be fixed to calculate a curve at a specific current density. Six of these are characteristics for the material used in the air electrode ($\bar{D}_g$, $\bar{D}_e$, $\bar{\kappa}$, $\bar{\kappa}_m$, γi_0, α), three parameters determine the experimental conditions (P_0, k, T) and four parameters fix the geometry of the air electrode (x_0, r_0, d_0, β). The parameters which are experimentally

determined for an electrode are the diffusion coefficient, $\bar{D}_g$, the electronic conductivity of the hydrophobic material, $\bar{\kappa}_m$, the ionic conductivity of electrolyte in the porous catalyst particles, $\bar{\kappa}$, the exchange current density per unit volume of the cylinder, γi_0, and the transfer coefficient, α. The effective diffusion coefficient in the electrolyte can be derived from conductivities $\bar{\kappa}$ and $\bar{\kappa}_m$. All the other parameters are known.

6.1. Measuring the diffusion coefficient of oxygen in the hydrophobic zone

At high current densities the diffusion coefficient in the hydrophobic zone is the most decisive factor. When the current density is increased, the concentration of the reactant is decreased at the surface of the cylinder. And finally with a specific current density the concentration approaches zero and the desired reaction can no longer take place. This current density is called the limiting current density and it can be measured.

After determining the limiting current density experimentally, the diffusion coefficient can be calculated from eqn. (9), which presents the limiting current density as a function of the effective diffusion coefficient at the hydrophobic zone. For the materials used in our air electrodes we have measured values $\bar{D}_g = 0.9 \times 10^{-6} \dots 7 \times 10^{-6}$ m^2/s, depending on the porosity of the hydrophobic zone. The preparation of our air electrodes is discussed in more detail in connection with the results.

6.2. Estimation of the diffusion coefficient of oxygen in the cylinder

The correlation between D_e, which is the diffusion coefficient of oxygen in pure electrolyte, and $\bar{D}_e$ can be given as

$$\bar{D}_e = \epsilon D_e \tag{44}$$

where ϵ is the diffusion resistance coefficient due to the porous structure. Knowing ϵ and D_e, the effective diffusion coefficient $\bar{D}_e$ can be calculated.

In connection with the theoretical estimation of ionic conductivity, it is shown that the diffusion resistance coefficient is related to the effective ionic conductivity, $\bar{\kappa}$, as follows

$$\epsilon = \frac{\bar{\kappa}}{\kappa} \tag{45}$$

6.3. Measuring the exchange current density and the transfer coefficient

These two parameters can be determined using very small total current densities. The local current density is given by eqn. (2). If the total current density is very small, it can be assumed that the concentration of oxygen remains constant throughout the cylinder, that the electronic IR drop is zero, $\eta_m(x) = 0$, and it can also be assumed that $\eta(x)$ is constant, $\eta(x_0)$. (When the current density is close to zero, electric field is also close to zero and it follows that $\eta(x)$ is almost a constant, since $j = \kappa E = -\kappa(\mathrm{d}\eta/\mathrm{d}x)$.) On the basis of these assumptions the local current density is

$$i(r,x) = i_0 \exp\left[\frac{\alpha z F}{RT} \eta(x_0)\right] \tag{46}$$

The total current density is presented by eqns. (3) and (5). When eqn. (46) is taken into account and when the double integration of eqn. (3) is calculated, the equation for total current density becomes

$$I = \gamma i_0 (1 - \beta) x_0 \exp\left[\frac{\alpha z F}{RT} \eta(x_0)\right] \tag{47}$$

From this equation the overpotential can be calculated

$$\eta(x_0) = \frac{RT}{\alpha z F} \ln(I) + \frac{RT}{\alpha z F} \ln(1/I_0) \tag{48}$$

where we have used the notation $I_0 = \gamma i_0 (1 - \beta) x_0$. When β, x_0 and I_0 are known, the characteristic parameter, γi_0, can be calculated. The current density I_0 can be determined experimentally. If the overpotential $\eta(x_0)$ is measured using very small current densities and these results are presented as a function of $\ln(I)$, the current density I_0 is the current density at $\eta(x_0) = 0$.

The transfer coefficient α is included in the gradient of this curve and it could be calculated from the term $RT/(\alpha z F)$, assuming that the stoichiometric number z is known. Actually, however there is no need to determine the transfer coefficient α and z separately, as only the product αz is needed, and it can be determined from the gradient of the curve. For a special catalyst, CoTMPP, we have measured values $\alpha z = 0.71 \ldots 1.37$.

6.4. Measuring the electronic conductivity of hydrophobic material

The conductivity can be determined using a rectangular sample of hydrophobic material, which is prepared by the same method as the air electrode. A known current, j, is conducted through the sample and the potential, U, is measured between two contacts, the distance between these contacts being d. The sample has a cross-sectional area of A, which should be constant throughout the sample. Now the current density is $I = j/A$, and using Ohm's law, the conductivity can be calculated

$$j/A = \bar{\kappa} E = \bar{\kappa} U/d \qquad \text{i.e. } \bar{\kappa} = jd/(AU) \tag{49}$$

For our base material (carbon 70 wt.% and PTFE 30 wt.%) we have measured values $\bar{\kappa}_m = 100 \ldots 360\ 1/(\Omega m)$.

6.5. Measuring the ionic conductivity of electrolyte in the cylinder

The material of the sample used for measurement is the catalyzed hydrophilic material used in the air electrode. The sample is in the electrolyte between two plates, through which the current is conducted. The potential difference across the sample is measured. When the thickness (d) and the cross-sectional area (A) of the sample are known, the effective ionic conductivity of electrolyte in the hydrophilic material can be calculated from

eqn. (49). We have not measured the ionic conductivity, but estimated it theoretically in the following way.

7. Theoretical estimation of ionic conductivity of electrolyte in the cylinder

First we consider the ionic conductivity of pure electrolyte. Let the electrode be a planar electrode and the electrolyte a KOH solution. We assume that there is enough oxygen available in the electrolyte for the reaction and also that there is no electrolyte convection. At first the concentration of K^+ and OH^- ions is assumed to be constant throughout the electrolyte. When a current density I is conducted through the electrode, the concentrations of the ions will change as a function of time and as a function of distance from the planar electrode, and the electric field is formed. The following equations describe the phenomena

$$\frac{\partial C_{OH}(x,t)}{\partial t} = D_{OH}\frac{\partial^2 C_{OH}(x,\,t)}{\partial x^2} + \frac{z_{OH}FD_{OH}}{RT}\frac{\partial(EC_{OH}(x,t))}{\partial x} \tag{50}$$

$$\frac{\partial C_K(x,t)}{\partial t} = D_K\frac{\partial^2 C_K(x,t)}{\partial x^2} + \frac{z_K FD_K}{RT}\frac{\partial(EC_K(x,t))}{\partial x} \tag{51}$$

$$\frac{dE(x,t)}{dx} = \frac{F}{\epsilon_0\epsilon_r}\sum_i (z_iC_i(x,t)) \tag{52}$$

The concentrations of K^+ and OH^- ions are denoted by $C_K(x,t)$ and $C_{OH}(x,t)$ and the diffusion coefficients by D_K and D_{OH}. E is the strength of the electric field, ϵ_0 is the permittivity of free space, ϵ_r is the dielectric constant of the medium and z_i is the charge of the ion. Equations (50) and (51) are the balance equations for OH^- ions and K^+ ions, respectively. Equation (52) is the first of the Maxwell equations.

The initial conditions are

$$C_{OH}(x,0) = C_{OH}^*, \quad C_K(x,0) = C_K^*, \quad E(x,0) = 0, \quad x \geqslant 0 \tag{53}$$

where C_i^* is the initial (bulk) concentration of ion i. And the boundary conditions are

$$j_{OH}(0,t) = -\frac{I}{F}, \quad j_K(0,t) = 0, \quad E(0,t) = 0, \quad t \geqslant 0 \tag{54}$$

where j_i is the flux of ion i as a function of distance and time. The condition for the strength of the electric field follows from the assumption that the electric conductivity of the planar electrode is sufficiently high for the field to remain at zero at the surface of the electrode.

Equations (50) - (52) are solved using the predictor-corrector method. This means that at each time, t_i, the concentrations and the induced electric

field are calculated until the change is small enough, thus the correct values of concentrations and strength of the electric field are attained at the time t_i. The time step Δt (= $t_i - t_{i-1}$) used in the calculations must be very small (10^{-11} s). Since it is a time-consuming process to calculate one time step, only about a thousand time steps can be calculated in a reasonable time. Thus, only time intervals of 10^{-9} s have been calculated. But this time interval proved to be sufficiently long to determine the strength of the electric field. This means that regarding the electric field the steady state is reached in less than 10^{-9} s.

When one thousand steps were calculated, it was found that the strength of the electric field reached a constant value very rapidly, after only a few time steps. Thus, by calculating only a small time interval, the induced electric field at a certain current density can be determined. It was also found that the strength of the electric field is constant throughout the electrolyte, except at the surface of the electrode, where its value is zero, as was assumed.

When the strength of the electric field is known, the ionic conductivity of the electrolyte can be determined; $\kappa = I/E$. If we assume that the diffusion coefficient is not dependent on the concentration, a linear dependency, $\kappa = \kappa(C)$, is attained (Fig. 4), which is not true in a real system. Experimentally determined [3] dependency between the ionic conductivity and the concentration of the electrolyte is also presented in Fig. 4. The deterioration of the conductivity at large concentrations can be explained by the dependency of the diffusion coefficient on the (bulk) concentration. The conductivity versus concentration is calculated by using the following diffusion coefficients

Ionic conductivity of KOH-electrolyte (1/(Ohm·cm))

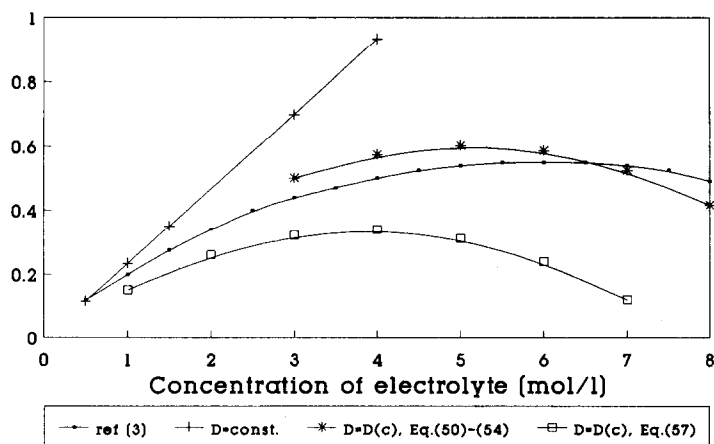Fig. 4. Ionic conductivity of KOH electrolyte.

$$D_{OH} = -6 \times 10^{-13} \left(\frac{m^5}{s\ mol} \right)(C_{OH}{}^* - 100\ mol/m^3) + 0.46 \times 10^{-8}\ m^2/s$$

$$D_{K} = -6 \times 10^{-13} \left(\frac{m^5}{s\ mol} \right)(C_{K}{}^* - 100\ mol/m^3) + 0.76 \times 10^{-8}\ m^2/s \qquad (55)$$

These are used when $C_i{}^* \geqslant 100\ mol/m^3$. When the concentrations are lower, values $D_{OH} = 0.46 \times 10^{-8}\ m^2/s$ and $D_K = 0.76 \times 10^{-8}\ m^2/s$ are used. The ionic conductivities based on these diffusion coefficients coincide well with the experimental curve (see Fig. 4).

Calculations also showed that the gradients of concentrations of OH^- and K^+ ions are zero throughout the electrolyte except in the immediate vicinity of the surface.

An approximate function for conductivity *versus* concentration can also be derived from the flux equation

$$J = -D \frac{dC}{dx} + \frac{zFD}{RT} CE \qquad (56)$$

We assume that only OH^- ions conduct the electricity in the steady state; the role of K^+ ions is only to maintain the electrical neutrality of the electrolyte.

We now know that the concentration has a gradient only in the vicinity of the surface of the electrode. Thus, only slightly farther away gradient dC/dx is zero. And when the flux is expressed by the current density ($J = I/(zF)$), we obtain the following equation

$$\kappa = \frac{I}{E} = \frac{z^2 F^2 D}{RT} C \qquad (57)$$

If the diffusion coefficient of eqn. (55) is used, we obtain from eqn. (57) a curve which resembles the experimentally determined curve (Fig. 4).

Now we consider a porous structure filled with electrolyte. The mathematics are still the same as described above, but we must use effective diffusion coefficients, $\bar{D}$. Now we can write an equation similar to eqn. (57), but κ and D are replaced by effective values, $\bar{\kappa}$ and $\bar{D}$. If these two equations are divided by each other, we obtain an equation for the effective diffusion coefficient of the OH^- ion

$$\bar{D} = \frac{\bar{\kappa}}{\kappa} D \qquad (58)$$

With $\epsilon = 0.045$ and using Fig. 4 we obtain $\bar{\kappa} = 2.5\ 1/(\Omega m)$ for 7 M KOH electrolyte.

Although eqn. (58) applies to the diffusion coefficient of the OH^- ion, it is obvious that this is also valid for the diffusion coefficient of oxygen in electrolyte, since both the OH^- ions and oxygen move in the electrolyte in the cylinder where they both have the same diffusion resistances. If we

compare eqns. (44) and (58) we can see that the diffusion resistance coefficient $\epsilon = \bar{\kappa}/\kappa$. Thus we can determine the effective diffusion coefficient of oxygen simply by measuring the effective conductivity of the electrolyte.

8. Results

A program has been made which calculates polarization curves with the given 13 parameters; the program solves eqns. (41) and (42) numerically. With this program the optimum geometry of the air electrode has been determined and the effects of the characteristic parameters on the performance of the electrode have been studied. Also, a calculated polarization curve has been fitted with a measured curve, and different possibilities for improving the performance of this air electrode made in our laboratory have been studied.

In these calculations the parameters which determine the circumstances are always the same; the initial partial pressure of oxygen $P_0 = 21\,280$ Pa, temperature $T = 298$ K and Henry's constant $k = 9.75 \times 10^{-7}$ mol/(m^3 Pa).

8.1. Optimization of geometrical parameters of the air electrode

In the following calculations the geometrical parameters have been optimized. The characteristic parameters which are used are:

$\bar{\kappa} = 2.5 \; 1/(\Omega\text{m})$

$\bar{\kappa}_\text{m} = 250 \; 1/(\Omega\text{m})$

$\bar{D}_\text{g} = 0.9 \times 10^{-6} \; \text{m}^2/\text{s}$

$\bar{D}_\text{e} = 2.2 \times 10^{-11} \; \text{m}^2/\text{s}$

$\gamma i_0 = 9.5 \times 10^5 \; \text{A/m}^3$

$RT/(\alpha z F) = 0.01901 \; \text{V}$

From Figs. 5 - 8 we can see that the optimum geometry for this particular air electrode at current density of 500 mA/cm^2 is

$x_0 = 0.05$ mm; $r_0 = 0.005 \; \mu\text{m}$; $d_0 = 0.0$ mm; $\beta = 0.4$.

We can also see from these Figures that the optimum geometry is different at smaller current densities. For example, at 100 mA/cm^2 the optimum length of the cylinder is between 0.15 and 0.2 mm. The optimum geometry is also dependent on the characteristic parameters. Thus, for each electrode with different characteristic parameters, the optimization must be done separately.

8.2. The effects of characteristic parameters on the performance of the air electrode

The contributions of the different characteristic parameters to the performance of the air electrode can be analyzed with the help of our program.
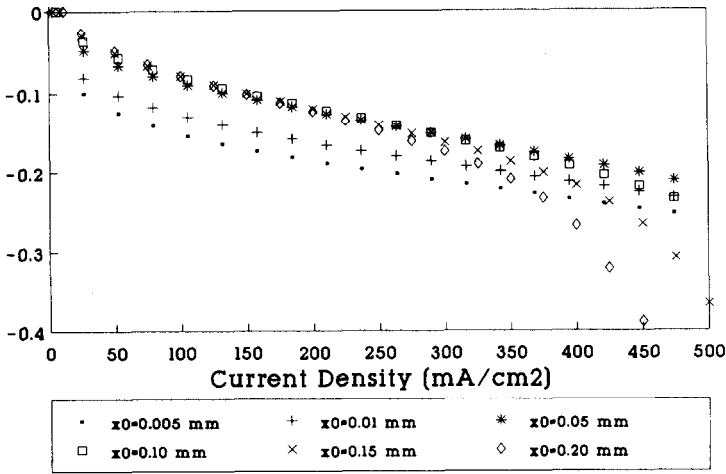
Potential vs. Hg/HgO (V)

·	x0=0.005 mm	+ x0=0.01 mm	*	x0=0.05 mm
□	x0=0.10 mm	× x0=0.15 mm	◊	x0=0.20 mm

Fig. 5. Polarization curves with different values of the length of the cylinder, x_0. The other geometrical parameters used are $r_0 = 0.15$ μm, $d_0 = 0.4$ mm, $\beta = 0.4$.

Potential vs. Hg/HgO (V)

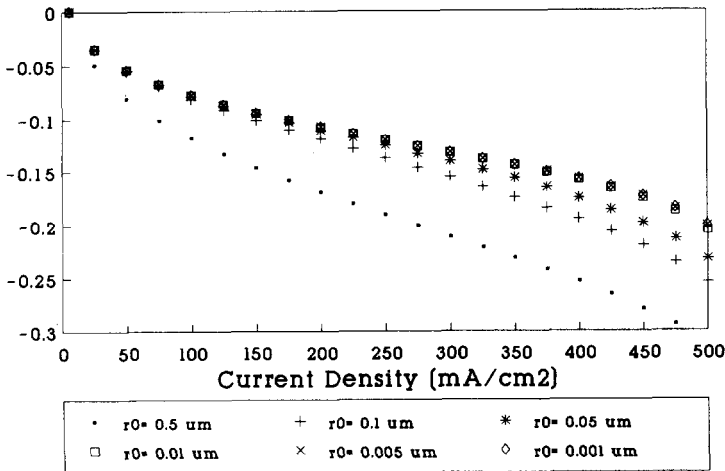|				
·	r0= 0.5 um	+ r0= 0.1 um	*	r0= 0.05 um
□	r0= 0.01 um	× r0= 0.005 um	◊	r0= 0.001 um

Fig. 6. Polarization curves with different values of the radius of the cylinder, r_0. The other geometrical parameters used are $x_0 = 0.1$ mm, $d_0 = 0.4$ mm, $\beta = 0.4$.

This is done by eliminating the effects of the other characteristic parameters. The geometrical parameters are fixed in all these cases; $x_0 = 0.1$ mm, $r_0 = 0.15$ μm, $d_0 = 0.4$ mm and $\beta = 0.4$. The parameters which determine the circumstances are as mentioned before.

To analyze the contribution of the electrochemical reaction of which the exchange current per unit volume $\gamma i_0 = 9.5 \times 10^{-5}$ A/m^3 and the slope
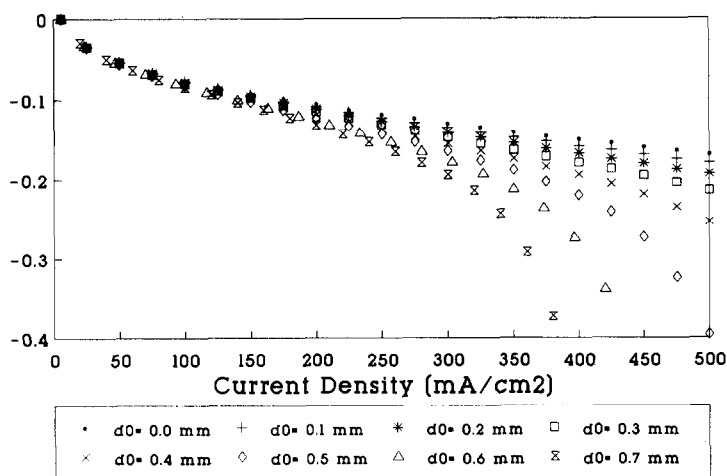
Potential vs. Hg/HgO (V)

Fig. 7. Polarization curves with different values of the thickness of the gas-supplying layer, d_0. The other geometrical parameters used are $x_0 = 0.1$ mm, $r_0 = 0.15$ μm, $\beta = 0.4$.
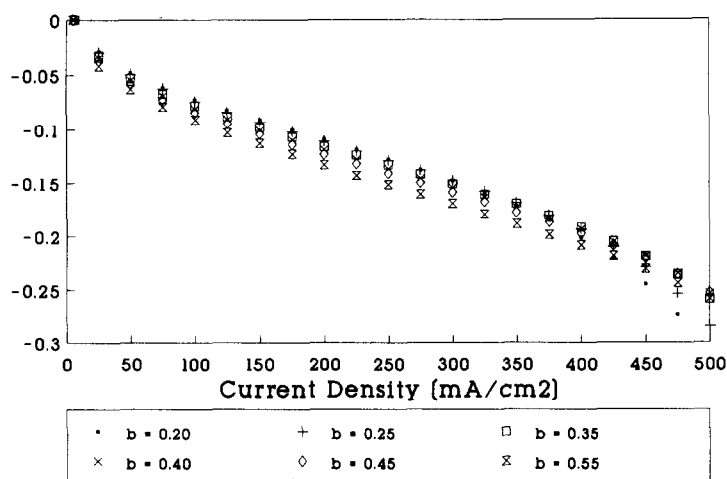
Potential vs. Hg/HgO (V)

Fig. 8. Polarization curves with different values of the void fraction, β. The other geometrical parameters used are $x_0 = 0.1$ mm, $r_0 = 0.15$ μm, $d_0 = 0.4$ mm.

$RT/(\alpha z F) = 0.01901$ V, the diffusion coefficients and the conductivities must have sufficiently high values so that there are no potential drops due to these factors; $\bar{\kappa} = 10\,000$ $1/(\Omega\text{m})$, $\bar{\kappa}_m = 10\,000$ $1/(\Omega\text{m})$, $\bar{D}_g = 1 \times 10^{-3}$ m^2/s and $\bar{D}_e = 1 \times 10^{-3}$ m^2/s. The polarization curve with these parameters is presented in Fig. 9.
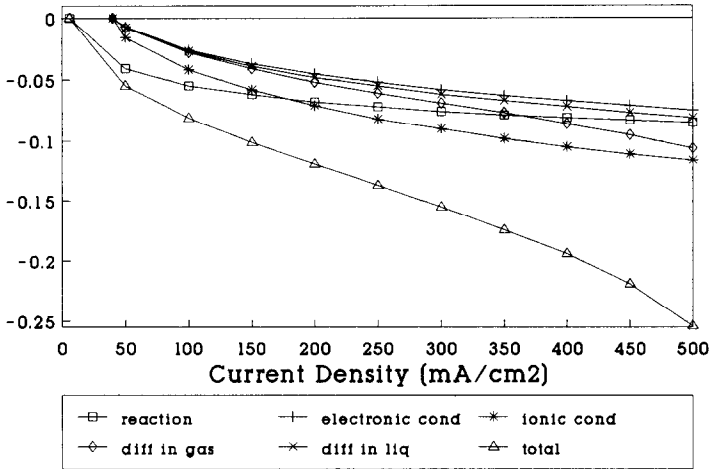
Potential vs. Hg/HgO (V)

Fig. 9. The contribution of the different factors to the performance of the air electrode.

In the case of the ionic and electronic conductivity, the diffusion coefficients are as before, the exchange current per unit volume $\gamma i_0 = 6.66 \times 10^6$ A/m^3 and the slope $RT/(\alpha z F) = 0.0257$ V ($\alpha = 0.5$, $z = 4$). The effects of these two conductivities are analyzed separately. For ionic conductivity analysis the parameters are: $\bar{\kappa} = 2.5\ 1/(\Omega m)$ and $\bar{\kappa}_m = 10\ 000\ 1/(\Omega m)$, and for the electronic conductivity analysis: $\bar{\kappa} = 10\ 000\ 1/(\Omega m)$ and $\bar{\kappa}_m = 250\ 1/(\Omega m)$. These curves are presented in Fig. 9.

The contributions of the effective diffusion coefficients of oxygen are also analyzed separately. The parameters used are: $\bar{\kappa} = 10\ 000\ 1/(\Omega m)$, $\bar{\kappa}_m = 10\ 000\ 1/(\Omega m)$, $\gamma i_0 = 6.66 \times 10^6$ A/m^3 and $RT/(\alpha z F) = 0.0257$ V. In the case of diffusion in the gas-supplying layer we have $\bar{D}_g = 0.9 \times 10^{-6}$ m^2/s and $\bar{D}_e = 1 \times 10^{-3}$ m^2/s and in the case of diffusion in the electrolyte: $\bar{D}_g = 1 \times 10^{-3}$ m^2/s and $\bar{D}_e = 2.2 \times 10^{-11}$ m^2/s (Fig. 9).

Although these factors can be analyzed separately, they are not independent of each other. In other words, we cannot take a sum of these curves to achieve the polarization curve where all these factors are considered, which is also presented in Fig. 9.

From Fig. 9 we can see that the most important factors which reduce the performance at low current densities (100 mA/cm^2) are the reaction itself and the ionic conductivity of the electrolyte, and at large current densities (500 mA/cm^2), the effective diffusion coefficient of oxygen in the gas-supplying layer and again the ionic conductivity. Thus, to increase the performance of this particular air electrode at low current densities, we should concentrate on catalyst research to improve the reaction mechanism. And if we want to improve the performance at large current densities, we should concentrate on decreasing the diffusion resistances in the gas-supplying layer, to make the electrode more porous.

We could also improve the effective ionic conductivity of the electrolyte in the catalyzed carbon agglomerate (in the cylinder). Since the electrolyte is 7 M KOH solution and its ionic conductivity is at its maximum, the only possibility for improving this parameter is to make the agglomerate more porous.

8.3. Simulation and comparison

In our laboratory we have made air electrodes consisting of two layers; a hydrophobic gas diffusion layer and the reaction layer, which is partly hydrophobic and partly hydrophilic. The hydrophilic material in the reaction layer consists of catalyzed carbon particles, which are flooded with electrolyte. The current collector grid is also embedded in the gas-supplying layer. This structure is very similar to the structure of the model electrode, and the program which was made can be used to optimize the structure of the electrode and also to analyze the contributions of the different factors to the performance of the real air electrode.

Both layers of the electrodes are made of a mixture of heat-treated carbon and PTFE powder. To prepare the gas-supplying layer the carbon (e.g., Vulcan XC-72R) was heat treated (900 °C, CO_2, 1/2 h) and mixed with Teflon dispersion (Du Pont Teflon resin 30N). The mixture was dried, ground and mixed again with organic solvent and NH_4HCO_3. After filtering this mixture it was rolled. The reaction layer was prepared in the same way, except that the catalyst was deposited onto the carbon after the heat treatment. After these two layers had been rolled separately, they were rolled together on the nickel-metal screen. The electrode was dried and then sintered in a furnace at 350 °C for 1/2 h. The preparation of the air electrode is discussed in more detail elsewhere [4].

The polarization curves were measured at room temperature using a 7 M KOH solution and an Hg/HgO reference electrode. There was no gas feeding to the air electrode, so that the partial pressure of oxygen was 0.21 atm. A measured curve is presesented in Fig. 10.

To simulate the real air electrode, all the characteristic parameters and the parameters which fix the experimental conditions must be known. Some of the geometrical parameters are also known; the thickness of the gas-supplying layer, the length of the cylinder which is the thickness of the reaction layer and the void fraction. Using the preparation method described briefly above, we can easily control all these three geometrical parameters, but the radius of the cylinder must be fitted with the measured curve. The known parameters of this real air electrode are:

$\bar{\kappa} = 2.5 \ 1/(\Omega m)$ $\qquad\qquad x_0 = 0.1$ mm

$\bar{\kappa}_m = 250 \ 1/(\Omega m)$ $\qquad\qquad d_0 = 0.4$ mm

$\bar{D}_g = 0.9 \times 10^{-6} \ m^2/s$ $\qquad\qquad \beta = 0.4$

$\bar{D}_e = 2.2 \times 10^{-11} \ m^2/s$ $\qquad\qquad P_0 = 21\,280$ Pa
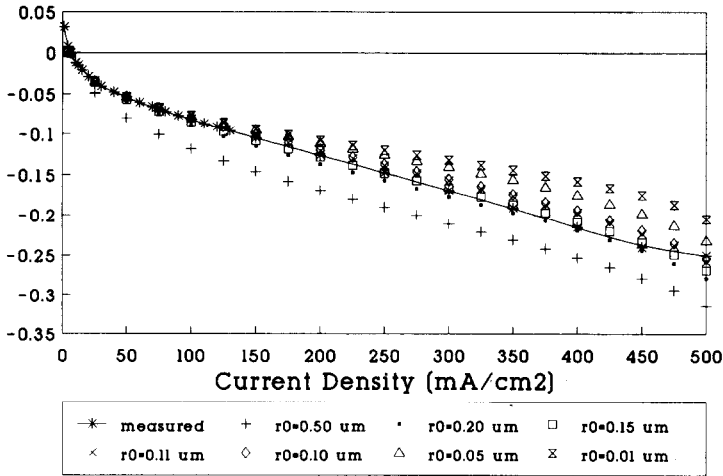
Potential vs. Hg/HgO (V)

Fig. 10. Measured polarization curve and calculated curves with different values of the radius r_0.

$\gamma i_0 = 9.5 \times 10^5 \, \text{A/m}^3$ $T = 298 \, \text{K}$

$RT/(\alpha z F) = 0.01901 \, \text{V}$ $k = 9.75 \times 10^{-7} \, \text{mol/(m}^3 \, \text{Pa)}$

Several polarization curves are calculated with these parameters, varying the value of the radius from 0.5 to 0.01 μm. These curves are also presented in Fig. 10, from which we can see that the calculated and the measured curve fit best when the radius is 0.15 μm.

The optimum geometry of this electrode has already been determined in Section 8.1; the same parameters were used in that connection. From Figs. 5 - 8 we can see that the performance of the air electrode could be improved by reducing the thickness of the reaction layer to 0.05 mm, by reducing the radius to 0.01 μm or by reducing the thickness of the gas-supplying layer as much as possible. The polarization curve for the air electrode in question with the optimum geometry is presented in Fig. 11.

The performance could also be improved by increasing the effective diffusion coefficient of oxygen in the gas-supplying layer, the electronic conductivity of the material or the activity of the catalyst. It is calculated how much improving these factors can affect the performance of the air electrode. The absolute maximum of the effective diffusion coefficient of oxygen in the gas-supplying layer is $20.8 \times 10^{-6} \, \text{m}^2/\text{s}$, which is the value in air with no diffusion resistances. The polarization curve is calculated with this diffusion coefficient, the other parameters being as mentioned for the real air electrode. Similarly, the polarization curves are calculated separately with values: $\bar{\kappa} = 10\,000 \, 1/(\Omega\text{m})$, $\alpha = 0.5$ and $\gamma_{i_0} = 6.66 \times 10^6 \, \text{A/m}^3$. A curve where all these values are used is also calculated and further, if we use the optimum geometry with these characteristic parameters an even better curve
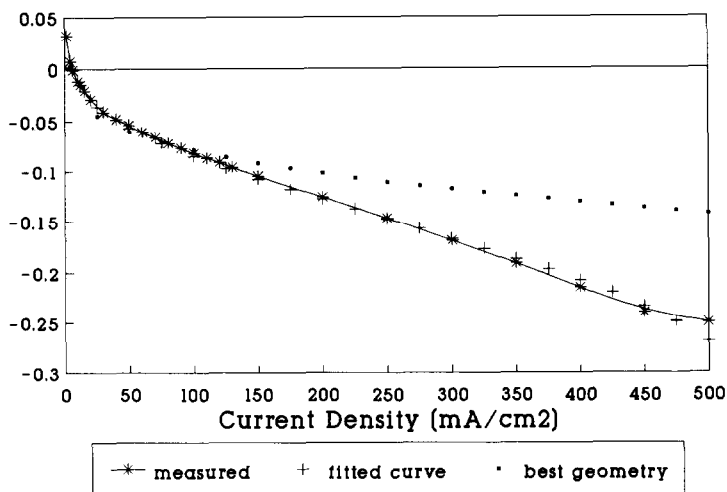
Potential vs. Hg/HgO (V)

Fig. 11. The measured polarization curve and calculated curve with optimum geometry.

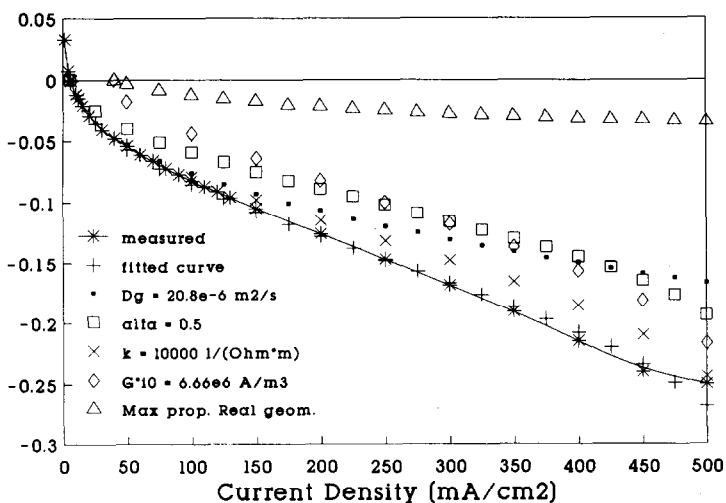## Potential vs. Hg/HgO (V)

Fig. 12. The effect on the performance of improving the characteristic parameters of the air electrode.

can be obtained (Fig. 12). But since most of the above mentioned characteristic parameters are impossible to reach in practice, the best curve is also the absolute upper limit for the performance of this electrode as long as the experimental conditions remain unchanged.

List of symbols

Roman symbols

C_0	Concentration of dissolved oxygen in the cylinder at equilibrium (mol/m^3)
C	Concentration of dissolved oxygen in the cylinder (mol/m^3)
C_1, C_2	Potential drops due to contacts (V)
d_0	Thickness of the gas supplying layer (m)
D_g	Diffusion coefficient of oxygen in gas $(mol/(Pa\ m\ s))$
$\bar{D}_g$	Effective diffusion coefficient of oxygen in the hydrophobic zone $(mol/(Pa\ m\ s))$
D_e	Diffusion coefficient of oxygen in pure electrolyte (m^2/s)
$\bar{D}_e$	Effective diffusion coefficient of oxygen in the cylinder (m^2/s)
E	Strength of the electric field (V/m)
F	Faraday constant (C/mol)
i_0, i_0'	Exchange current density (A/m^2)
i	Local current density (A/m^2)
I	Total current density (A/m^2)
I_{lim}	Limiting current density (A/m^2)
I_0	Modified Bessel function in connection with solving the equations
I_0	Current density, defined as $\gamma i_0(1-\beta)x_0$ (A/m^2)
I_1	Modified Bessel function of the first order
j	Current (A)
j_L	Ionic current (A)
j_M	Electronic current (A)
J	Flux of oxygen $(mol/m^2\ s)$
k	Henry's constant $(mol/m^3\ Pa)$
n	Number of electrons involved in the reaction
N	Number of elements per unit area (m^{-2})
P	Partial pressure of oxygen in the hydrophobic zone (Pa)
P_0	Initial partial pressure of oxygen at $x = -d_0$ (Pa)
q	Function defined by eqn. (38)
r_0	Radius of the cylinder (m)
R	Gas constant (J/mol K)
S	Cross-sectional area of an element surrounding the cylinder (m^2)
T	Temperature (K)
x_0	Length of the cylinder (m)
z	Stoichiometric number

Greek symbols

α	Transfer coefficient
β	Void fraction
ϵ	Diffusion resistance coefficient
ϵ_0	Permittivity of free space (F/m)
ϵ_r	Dielectric constant of the medium
ϕ_L	Potential in the liquid phase (V)

ϕ_M Potential in the solid material phase (V)

ϕ_{ref} Potential of the reference electrode (V)

ϕ_1 Potential of the working electrode at $x = -d_0$ (V)

ϕ_{M_0} Potential in the material when the electronic conductivity of the material is infinite (V)

η Overpotential (V)

η_m Overpotential due to the electronic IR drop (V)

γ Ratio of catalyst surface area to catalyst volume

$\bar{\kappa}$ Effective ionic conductivity of the electrolyte in the cylinder $(1/(\Omega m))$

$\bar{\kappa}_m$ Effective electronic conductivity of the material $(1/(\Omega m))$

References

1 J. Giner and C. Hunter, *J. Electrochem. Soc.*, *116* (1969) 1124.
2 I. Iliev, S. Gamburzev, A. Kaisheva, *J. Appl. Electrochem.*, *5* (1975) 291 - 297.
3 V. Kireev, *Physical Chemistry* (1979).
4 J. Kivisaari, J. Lamminen, M. J. Lampinen and M. Viitanen, *J. Power Sources*, *32* (1990) 233.